

Transient Behavior of the Dynamically Ordered Phase in Uniaxial Cobalt Films

A. Berger,¹ O. Idigoras,¹ and P. Vavassori^{1,2}

¹*CIC nanoGUNE, E-20018 Donostia-San Sebastian, Spain*

²*IKERBASQUE, The Basque Foundation for Science, E-48011 Bilbao, Spain*

(Received 14 June 2013; revised manuscript received 10 October 2013; published 4 November 2013)

We study the time dependent magnetic behavior of uniaxial cobalt films in the vicinity of the dynamic phase transition (DPT) as a function of the period P and bias H_b of an oscillating magnetic field. In addition to the DPT at a critical period P_c , we observe the occurrence of transient behavior for $P < P_c$. Our data can be consistently explained by the existence of a phase line at $H_b = 0$ for $P < P_c$, which causes a first order phase transition in between two antiparallel dynamic order states, thus indicating far-reaching similarities of the DPT to equilibrium phase transitions in ferromagnets.

DOI: [10.1103/PhysRevLett.111.190602](https://doi.org/10.1103/PhysRevLett.111.190602)

PACS numbers: 05.70.Ln, 64.60.-i, 75.60.Ej, 75.70.-i

Dynamic pattern formation and dynamically ordered states are important aspects of nature, scientific phenomena, and even daily life, given that fluid dynamics, laser emission, and human brain activity are all reliant on spatiotemporal pattern formation and their predictable time evolution [1–4]. Other prominent examples include surface reactions, mechanical crack propagations, and self-organized criticality [5–8]. Correspondingly, wide-ranging research activities in this field are commonplace, including the theory and modeling of dynamic order and pattern formation [2], of which much is based on the insights of catastrophe theory [9].

One frequently used model in this field of research is the kinetic Ising model with ferromagnetic coupling J because already this simple model can exhibit qualitative changes in its dynamic behavior as one changes the external driving force in a continuous fashion. Upon applying a magnetic field oscillation of amplitude H_0 , the magnetization of the dynamic Ising model follows the cyclical external field for sufficiently slow field changes, but it is not able to do so anymore if the field oscillation period P becomes short in comparison to the relaxation time τ of the magnetic system. Hereby, it was observed that the time averaged magnetization value Q starts to deviate from zero at a specific period P_c , which marks a critical point and hereby a qualitative change in the system's dynamic response. For periods shorter than this critical period P_c , the time dependent magnetization oscillates only weakly around a nonvanishing Q value, which is the order parameter of this so-called dynamic ferromagnetic phase. Correspondingly, the strongly oscillating magnetization behavior observed for long periods $P > P_c$, for which Q averages to zero, is the dynamic paramagnetic phase. Prior theoretical work demonstrated that this model undergoes a dynamic phase transition (DPT) upon varying the period P of a time dependent magnetic field oscillation for all temperatures T below the Curie temperature T_C [10–13]. While many aspects of this dynamic phase transition have been studied in the past by means of theory or modeling [10–27],

including different dimensionalities and specific implementations of the kinetic Ising model [28], rather few experimental works have addressed this topic [29–33]. More importantly, in both experiment and theory the DPT has been investigated in a limited fashion, because only the P dependence of Q was studied for any given set of J , H_0 , and T . Only very few recent works consider the possibility of utilizing an additional time-independent bias field H_b to influence the dynamic phase and phase transition [19,23,25,33]. Hereby, H_b appears to be the conjugate field of the order parameter Q , so that its study would enable the exploration of a two-dimensional H_b - P phase space, analogous to the H - T phase space for ferromagnetism in thermal equilibrium [25]. Last, the exploration of the dynamically ordered phase in the entire H_b - P phase space should allow for the systematic investigation of transient behavior that has not at all been addressed so far, with the exception of critical slowdown in the dynamic paramagnetic phase [12,13,21]. The investigation and determination of transient behavior should be most relevant for dynamically ordered states, because it is the limited ability of physical systems to follow external forces that causes the multiplicity of dynamically ordered states in the first place [11–13]. In this work, we address exactly these aspects by performing an experimental study on a suitable ferromagnetic film system, utilizing H_b and P as tunable external input variables.

With respect to the sample, the extensive theoretical and modeling work [10–27] gives very clear guidelines in that the sample should be uniaxial as well as have no or only minimal dipolar demagnetization effects, because otherwise the tendency towards magnetic bistability is suppressed [34]. Thus, a thin film geometry with a single easy axis of magnetization within the film plane is ideal. Correspondingly, we have grown 30 nm thick Co films with (10 $\bar{1}$ 0) texture by means of sputter deposition onto Ar plasma etched Si(110) substrates [35]. Here, the specific growth sequence to achieve good texture with an in-plane aligned hcp c axis was Cr 25 nm/Co 30 nm, upon which

10 nm SiO₂ were deposited for oxidation protection. Our specific growth process was optimized to achieve a high magnetic orientation ratio [36], i.e., a high degree of uniaxial magnetic alignment, while keeping the coercive field low enough to facilitate our dynamic magnetic measurements.

The quasistatic magnetic properties of one sample are shown in Fig. 1. The main figure shows the magnetic hysteresis loop along the easy in-plane magnetization axis, which was measured by means of the longitudinal magneto-optical Kerr effect (L-MOKE). The measurement shows a perfectly square loop with flat branches and an abrupt magnetization transitions at the coercive field $\pm H_C$, highlighting the bimodal Ising model-like nature of our samples [37]. The pronounced uniaxial anisotropy is evident from the data shown in the inset, where the ratio of the remanent magnetization to saturation magnetization is shown as a function of the applied magnetic field angle β . The data show a clear 180° periodicity and are in near perfect agreement with the macrospin projection onto the field axis, shown as a solid line here. Thus, our samples show the key ingredients needed to experimentally study the dynamically ordered phase.

For our high sensitivity and broad bandwidth L-MOKE setup, we utilized an intensity and polarization stabilized diode laser with $\lambda = 532$ nm and 50 mW output power, a high quality polarizer, and a quarter-wavelength retarder plus Wollstone cube beam splitter in combination with a differential photodiode with on-chip amplifier to measure the MOKE ellipticity [38]. Overall, our L-MOKE setup enabled measurement of the Co-film saturation signal with a signal-to-noise ratio of 48.2 ± 0.2 in $30 \mu\text{s}$, thus allowing real-time full hysteresis loop measurements with

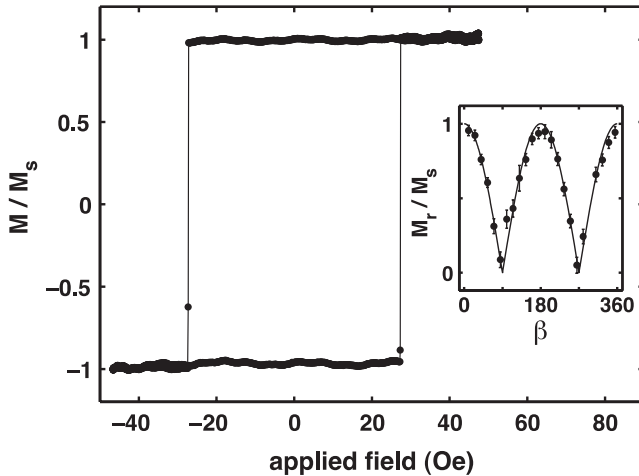


FIG. 1. Quasistatic hysteresis loop measurement along the easy axis of magnetization for a 30 nm Co film with in-plane uniaxial anisotropy; the inset shows the angular dependence of the remanent magnetization M_r , normalized to the saturation magnetization M_s . The black dots are the data, while the solid line represents the expected behavior for a perfect uniaxial system.

periods P of down to $600 \mu\text{s}$. Examples of the magneto-optically measured magnetization time traces are shown in Fig. 2 for a Co film upon applying an oscillatory field amplitude H_0 of 30.80 Oe at $P = 10$ ms. Hereby, Fig. 2(a) shows the signal without an applied bias field, while Fig. 2(b) displays a time trace for a relatively large bias field of $H_b = +1.40$ Oe. While the biased curve shows only a small magnetization variation, the unbiased curve shows a nearly rectangular shaped time sequence. So, while our Co-film system clearly exhibits a paramagnetic dynamic state with $Q = 0$ in Fig. 2(a) for the specific H_0 and P chosen here, the application of $H_b = 1.40$ Oe [Fig. 2(b)] is sufficient to induce a large Q value, similar to static paramagnetic saturation at very large applied fields. The fact, that a bias field of only 1.40 Oe can cause such high levels of Q highlights the absolute necessity of excellent magnetic field control [39]. At lower periods P , the sample is in the dynamically ordered phase and this H_b induced effect is much weaker because the expectation value of Q is already substantial without applying H_b , in close similarity to the magnetization vs magnetic field response in equilibrium for a ferromagnet below T_C [40].

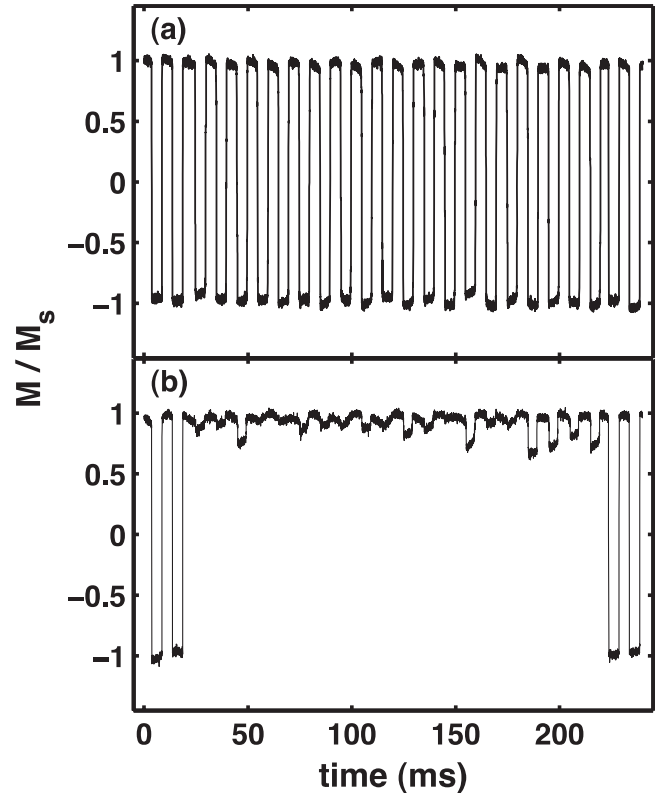


FIG. 2. L-MOKE signal time traces upon applying a sinusoidal magnetic field of amplitude $H_0 = 30.80$ Oe and $P = 10$ ms along the easy axis of magnetization. (a) Measurement without bias field H_b ; (b) measurement with $H_b = 1.40$ Oe. The first two and the last two field cycles are done at $H_0^{\text{ref}} = 50.00$ Oe to generate reference measurements with full magnetization reversal.

This limited H_b response can be seen in Figs. 3(a)–3(d), if one looks specifically at the Q data upon bias field reduction from its maximum value of $H_b = 1.20$ Oe to zero field. In this range, and for the H_0 and P values chosen here, Q shows only a small H_b dependent effect.

Overall, Fig. 3 shows experimental Q values that were averaged over $N = 50$ –400 cycles at constant H_b , after which H_b was changed to the next value in step sizes of 0.025 Oe. Data taken during H_b reduction from +1.20 Oe to -1.20 Oe are shown as dots, while data for H_b increase from -1.20 Oe to +1.20 Oe are shown as squares. The key observation here is that the dynamically ordered state is not simply inverted at $H_b = 0$, but instead shows transient behavior, in which the magnetization cycle dynamics shows a delayed and gradual approach to the stable dynamically ordered state. This leads to the occurrence of Q vs H_b hysteresis as seen in Fig. 3. Also, this hysteresis effect is reduced upon increasing the cycle number N , viz. measurement time for every Q data point. This trend is fully consistent with the data interpretation as transient behavior, because larger measurement times will reduce

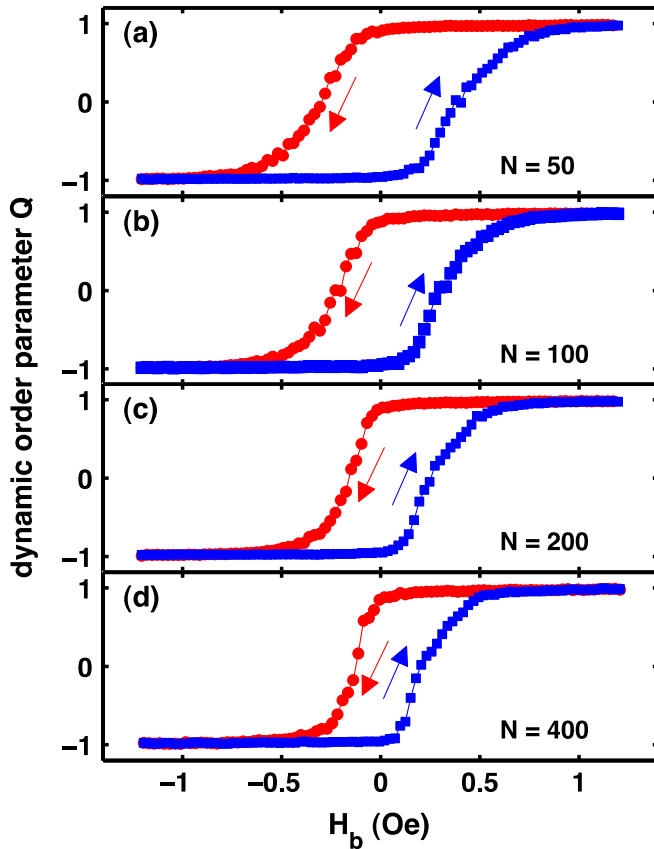


FIG. 3 (color online). H_b dependence of the dynamic phase order parameter Q measured for $H_0 = 29.80$ Oe and $P = 2.5$ ms. Measurements (a)–(d) differ in the number of oscillation field cycles N that were measured for every bias field step, prior to changing H_b . Data for decreasing and increasing H_b are shown as (red) dots and (blue) squares, respectively.

the relevance of transient dynamics. However, the behavior is not simply proportional to time, because an increase from 50 to 400 cycles does not reduce the transient H_b range by a factor of 8, but to a much lesser degree. Thus, the $1/N$ metafrequency dependence of the $Q(H_b)$ -hysteresis-loop width is far weaker than linear. This Q vs H_b behavior is very reminiscent of the M vs H behavior for quasistatic near-equilibrium ferromagnetism, where the inversion of an applied field H causes a crossing of the phase boundary at $H = 0$, which in turn produces the conventional hysteretic behavior of magnetization reversal [41]. Furthermore, this $M(H)$ behavior is generally found to be weakly dependent on the applied field frequency [29–31], just as we observed here a clearly visible, but weak $1/N$ metafrequency dependence for $Q(H_b)$. So, overall the $Q(H_b)$ behavior indicates that H_b is indeed the conjugate field to Q and that H_b changes cause transient behavior that is consistent with a phase boundary at $H_b = 0$.

To further investigate the occurrence of this transient behavior, we have studied its P dependence for different H_0 . Some representative results are displayed in Fig. 4. To generate the experimental plots in Fig. 4, we have measured the type of H_b -field cycles, shown in Fig. 3, for different P values, using $N = 250$. Figure 4(a) shows the measured stable dynamic order parameter Q as a function of P and H_b as a color-coded map for one particular H_0 value [42]. Here, we observe a sharp transition at $H_b = 0$ in between positive and negative Q values for $P < P_c = 3.5$ ms, thus indicating the above mentioned phase line. For larger periods, the transition in between positive and negative Q values is gradual with Q actually vanishing at $H_b = 0$. Thus, no phase line exists here and $P > 3.5$ ms corresponds to the paramagnetic dynamic phase. Figure 4(b) shows a map of $\Delta Q(H_b, P) = Q^d(H_b, P) - Q^i(H_b, P)$, which is the difference of the Q values measured for the decreasing H_b branch $Q^d(H_b, P)$ and the increasing H_b branch $Q^i(H_b, P)$. Thus, ΔQ differs from zero only in the hysteretic parts of the $Q(H_b)$ loops, which appear as the approximately triangular ΔQ -structure on the left-hand side of Fig. 4(b) extending up to the critical period P_c . For $P > 3.5$ ms, ΔQ is approximately zero independent from H_b . This is consistent with the fact that the transient behavior of Fig. 3 is intimately coupled with the dynamically ordered state in the same way, in which conventional magnetic hysteresis is limited to the ferromagnetic phase and its $H = 0$ phase boundary [43]. The approximate triangular shape for $P < 3.5$ ms in Fig. 4(b) means that there is an upper $|H_b|$ value for every P , above which no transient behavior is observed anymore on the time scale of the experiment and that the bistability regime increases as P moves away from the critical point at P_c .

Upon applying higher oscillation field amplitudes H_0 , one expects the ferromagnetic dynamic state to shift towards lower P values. Correspondingly, the bistability regime of $Q(P, H_b)$ should also shift, which is exactly what

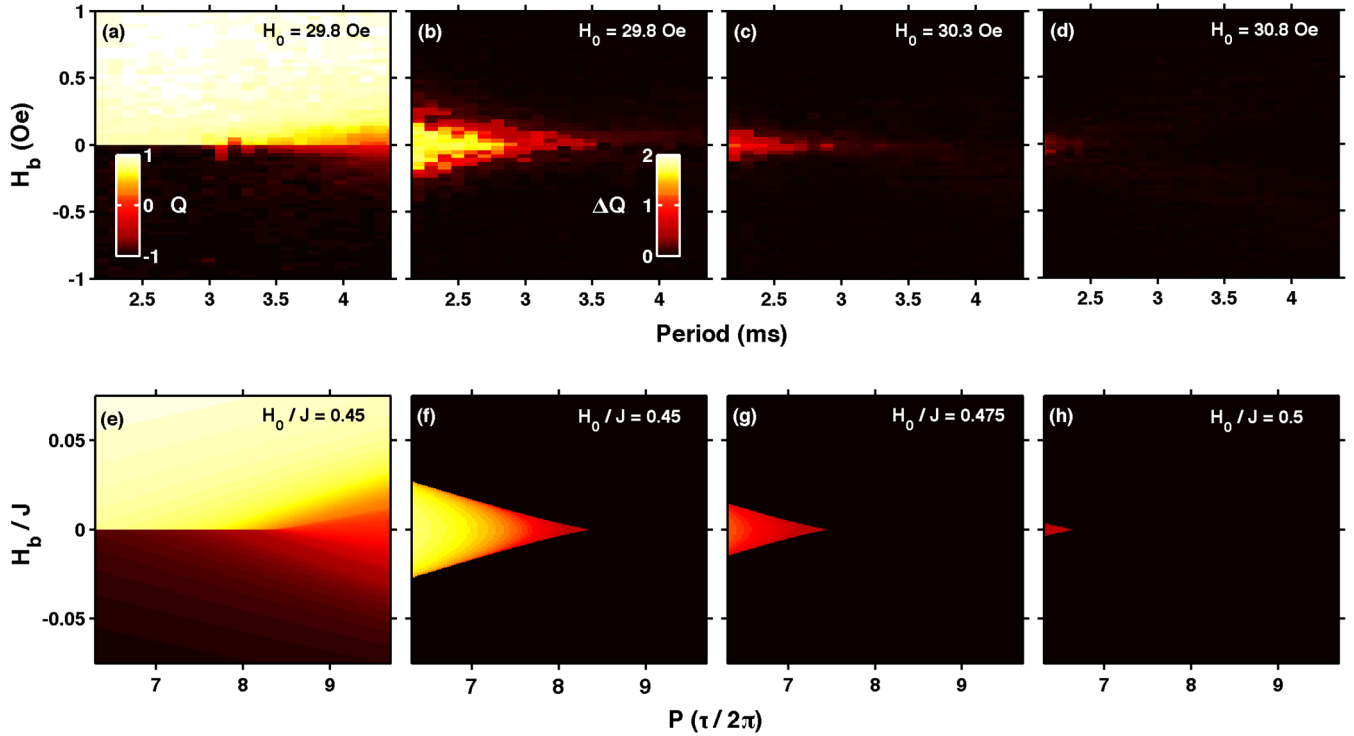


FIG. 4 (color online). Q and ΔQ data as a function of P and H_b displayed as gray-scale (color-coded) maps: (a)–(d) are experimental data, while (e)–(h) display the results of numerical simulations based upon the mean-field approximation [23]. (a) and (e) show the stable dynamic order parameter $Q(H_b, P)$. The gray scale (color code) shown in (a) applies to (a) and (e). (b)–(d) and (f)–(h) show $\Delta Q(H_b, P)$ for measurements and calculations with the corresponding gray scale (color code) for all figures displayed in (b) only. H_0 values are given in each map.

we observe in Figs. 4(c) and 4(d) with a shift of the triangular shaped $\Delta Q > 0$ structure to the left. Figures 4(e)–4(h) show the results of mean-field calculations for the purpose of a qualitative comparison with our experimental data [23]. Figure 4(e) shows the $Q(P, H_b)$ phase diagram that is described by the mean-field equation of state

$$Q^3 - A(P_c - P)Q - BH_b = 0 \quad (1)$$

in the vicinity of the critical point at $P = P_c$ and $H_b = 0$ [25]. Hereby, A and B are analytical functions that are weakly P and H_b dependent, making Eq. (1) a typical example of cusp shape catastrophe behavior [9]. As one can see from Fig. 4, the calculation results resemble our experimental data very well, even if the $Q \approx 0$ regime in the calculated paramagnetic dynamic phase [Fig. 4(e)] is larger than in our experiments [Fig. 4(a)], a fact that is explained by the different critical exponents predicted in mean field models [44]. We also followed metastable steady states for decreasing and increasing values of H_b and we observe $Q(H_b)$ hysteresis similar to our experiments. The existence of two stable dynamic states with opposite Q was already mentioned by Tomé and Oliveira [10], but the H_b dependence of this numerical stability has not yet been studied. We find that for $P < P_c$, there is an H_b range in which both dynamic states are numerically stable. We furthermore observe that, similar to our experiments, the bistability range increases

with decreasing P , thus producing the same type of triangular shape in Figs. 4(f)–4(h). Also, the H_0 -dependent shift of the bistability regime resembles the experimental observations very closely.

All of the above demonstrates that by using and exploring the H_b dependence of the order parameter Q , one has access to far more aspects of the physics that is underlying the dynamically ordered phase. We find that H_b appears to define a phase line at $H_b = 0$ for $P < P_c$, causing a first order phase transition in between two antiparallel but otherwise equivalent dynamic order states, that upon crossing also generates transient bistability of the order parameter and thus hysteresis. All of our results indicate that the similarities of the dynamic phase transition and the thermodynamic ferromagnetic phase transition are much further reaching than has been assumed so far.

We acknowledge funding from the Basque Government (Program No. PI2012-47) and the Spanish Government (Project No. MAT2012-36844). O.I. acknowledges the Basque Government for support from Grant No. BFI09.284.

-
- [1] G. Schoener and J. A. S. Kelso, *Science* **239**, 1513 (1988).
[2] M. C. Cross and P. C. Hohenberg, *Rev. Mod. Phys.* **65**, 851 (1993).

- [3] V. K. Jirsa and H. Haken, *Phys. Rev. Lett.* **77**, 960 (1996).
- [4] J. Kröll, J. Darmo, S. S. Dhillon, X. Marcadet, M. Calligaro, C. Sirtori, and K. Unterrainer, *Nature (London)* **449**, 698 (2007).
- [5] P. Bak, C. Tang, and K. Wiesenfeld, *Phys. Rev. A* **38**, 364 (1988).
- [6] S. Jakubith, H. H. Rotermund, W. Engel, A. von Oertzen, and G. Ertl, *Phys. Rev. Lett.* **65**, 3013 (1990).
- [7] D. Bonamy, S. Santucci, and L. Ponsou, *Phys. Rev. Lett.* **101**, 045501 (2008).
- [8] A. Shekhawat, S. Zapperi, and J. P. Sethna, *Phys. Rev. Lett.* **110**, 185505 (2013).
- [9] See, for instance, T. Poston and I. Stuart, *Catastrophe Theory and Its Application* (Pitman, New York, 1978).
- [10] T. Tomé and M. J. de Oliveira, *Phys. Rev. A* **41**, 4251 (1990).
- [11] B. K. Chakrabarti and M. Acharyya, *Rev. Mod. Phys.* **71**, 847 (1999).
- [12] G. Korniss, C. J. White, P. A. Rikvold, and M. A. Novotny, *Phys. Rev. E* **63**, 016120 (2000).
- [13] M. Acharyya, *Int. J. Mod. Phys. C* **16**, 1631 (2005).
- [14] M. Acharyya and B. K. Chakrabarti, *Phys. Rev. B* **52**, 6550 (1995).
- [15] M. Acharyya, *Phys. Rev. E* **56**, 1234 (1997).
- [16] S. W. Sides, P. A. Rikvold, and M. A. Novotny, *Phys. Rev. Lett.* **81**, 834 (1998).
- [17] M. Acharyya, *Phys. Rev. E* **59**, 218 (1999).
- [18] G. Korniss, P. A. Rikvold, and M. A. Novotny, *Phys. Rev. E* **66**, 056127 (2002).
- [19] D. T. Robb, P. A. Rikvold, A. Berger, and M. A. Novotny, *Phys. Rev. E* **76**, 021124 (2007).
- [20] S. Akkaya Deviren and E. Albayrak, *Phys. Rev. E* **82**, 022104 (2010).
- [21] M. Acharyya and A. B. Acharyya, *Int. J. Mod. Phys. Conf. Ser.* **21**, 481 (2010).
- [22] U. Akinci, Y. Yueksel, E. Vatansver, and H. Polat, *Physica (Amsterdam)* **391A**, 5810 (2012).
- [23] O. Idigoras, P. Vavassori, and A. Berger, *Physica (Amsterdam)* **407B**, 1377 (2012).
- [24] H. Park and M. Pleimling, *Phys. Rev. Lett.* **109**, 175703 (2012).
- [25] R. A. Gallardo, O. Idigoras, P. Landeros, and A. Berger, *Phys. Rev. E* **86**, 051101 (2012).
- [26] M. Ertas, B. Deviren, and M. Keskin, *Phys. Rev. E* **86**, 051110 (2012).
- [27] H. Park and M. Pleimling, *Phys. Rev. E* **87**, 032145 (2013).
- [28] Much of the theoretical work, including the pioneering work by Tome and Oliveira [10] is based on a model, in which all spins are coupled in an identical fashion to all other spins even in the limit of infinite system size. It is therefore intrinsically a mean-field model without being a mean-field approximation of an otherwise formulated Hamiltonian that represents a specific dimensionality. In contrast, most of the Monte Carlo simulation work was done for conventional next neighbor Hamiltonians in two-dimensional systems. Also, we understand our experimental Co films to represent two-dimensional systems as far that the dynamic phase transition is concerned, because the film thickness of 30 nm is too small to allow for depth dependent magnetization reversal states to occur in the frequency range of interest here.
- [29] Y. L. He and G. C. Wang, *Phys. Rev. Lett.* **70**, 2336 (1993).
- [30] Q. Jiang, H. N. Yang, and G. C. Wang, *Phys. Rev. B* **52**, 14911 (1995).
- [31] J.-S. Suen and J. L. Erskine, *Phys. Rev. Lett.* **78**, 3567 (1997).
- [32] W. Kleemann, J. Rhensius, O. Petravic, J. Ferre, J. P. Jamet, and H. Bernas, *Phys. Rev. Lett.* **99**, 097203 (2007).
- [33] D. T. Robb, Y. H. Xu, O. Hellwig, J. McCord, A. Berger, M. A. Novotny, and P. A. Rikvold, *Phys. Rev. B* **78**, 134422 (2008).
- [34] J. H. Carpenter, K. A. Dahmen, A. C. Mills, M. B. Weissman, A. Berger, and O. Hellwig, *Phys. Rev. B* **72**, 052410 (2005).
- [35] O. Idigoras, A. K. Suszka, P. Vavassori, P. Landeros, J. M. Porro, and A. Berger, *Phys. Rev. B* **84**, 132403 (2011).
- [36] Conventionally, the orientation ratio (OR) of a magnetic material is defined as the ratio of the remanent magnetization values, measured along the easy axis M_r (easy) vs the hard axis M_r (hard), i.e., $OR = M_r(\text{easy})/M_r(\text{hard})$; for further details, see, for instance, O. Idigoras, P. Vavassori, J. M. Porro, and A. Berger, *J. Magn. Magn. Mater.* **322**, L57 (2010).
- [37] For these types of samples, deviations from bimodal quasistatic behavior can occur, but only for magnetic field orientations that are sufficiently misaligned with respect to the easy axis. For a detailed study of this field angle behavior, see J. A. Arregi, O. Idigoras, P. Vavassori, and A. Berger, *Appl. Phys. Lett.* **100**, 262403 (2012).
- [38] J. M. Teixeira, R. Lusche, J. Ventura, R. Fermento, F. Carpinteiro, J. P. Araujo, J. B. Sousa, S. Cardoso, and P. P. Freitas, *Rev. Sci. Instrum.* **82**, 043902 (2011).
- [39] In addition to the very good sensitivity of our L-MOKE setup, we also use a specialized magnet with sintered ferrite yoke to insure minimal field amplitude and bias field variations. Specifically, we determined the root mean square (rms) noise level of H_0 and H_b to be 0.022 Oe.
- [40] C. Liu, E. R. Moog, and S. D. Bader, *Phys. Rev. Lett.* **60**, 2422 (1988).
- [41] See, for instance, G. Bertotti, *Hysteresis in Magnetism* (Academic, San Diego, 1998).
- [42] To generate Fig. 4(a), we have combined the Q measurements for positive decreasing H_b values with the equivalent results for negative increasing H_b values, so that only Q data that represent stable dynamic states are displayed.
- [43] See, for instance, N. D. Goldenfeld, *Lectures on Phase Transitions and the Renormalization Group* (Addison-Wesley, Reading, MA, 1992).
- [44] Also the absolute field scales of H_0 and H_b with respect to J are much smaller in the experiment than in the theoretical model. This can be qualitatively explained by the fact that the anisotropy in our experimental Co samples is far smaller than the exchange coupling constant. Correspondingly, domain wall and nucleation domain energies are substantially reduced if compared to Ising-like models, which then has to be counterbalanced by far smaller Zeeman energy contributions and thus far smaller magnetic field values.